Edge phonon state of mono- and few-layer graphene nanoribbons observed by surface and interference co-enhanced Raman spectroscopy

Wencai Ren,[1,*] Riichiro Saito,[2] Libo Gao,[1] Fawei Zheng,[2] Zhongshuai Wu,[1] Bilu Liu,[1] Masaru Furukawa,[2] Jinping Zhao,[1] Zongping Chen,[1] and Hui-Ming Cheng[1,†]

[1]*Shenyang National Laboratory for Materials Science, Institute of Metal Research, Chinese Academy of Sciences, 72 Wenhua Road, Shenyang 110016, People's Republic of China*

[2]*Department of Physics, Tohoku University, Sendai 980-8578, Japan*

(Received 23 August 2009; revised manuscript received 6 December 2009; published 12 January 2010)

Using surface and interference co-enhanced Raman scattering measurements, we detected two well-distinguished Raman bands at 1450 and 1530 cm^{-1} from individual mono- and few-layer graphene nanoribbons (GNRs) prepared by chemical exfoliation and mechanical cleavage of graphite. The intensities of these two peaks strongly depend on the width and edge structure of the GNRs. Combining with first-principles calculations, the 1450 and 1530 cm^{-1} Raman bands are assigned to the localized vibration of the edge atoms of zigzag and armchair GNRs terminated with H atoms, respectively. In addition, two weak peaks at ~1140 and 1210 cm^{-1} are also observed, which are coupled with 1450 and 1530 cm^{-1}, respectively. These findings enrich the understanding on the fine structure of mono- and few-layer GNRs by Raman spectroscopy.

DOI: 10.1103/PhysRevB.81.035412 PACS number(s): 61.48.De, 33.20.Fb, 63.20.D−, 78.30.−j

I. INTRODUCTION

Graphene nanoribbons (GNRs), narrow stripes of graphene with a width typically smaller than 100 nm, have recently attracted extensive interests because of their unique structure-dependent electronic properties and promising applications in nanoelectronics and spintronics.[1–8] Theoretical calculations indicate that GNRs display a variety of electronic properties depending on their width and edge structure.[2–4,7,8] Previous studies show that GNRs with an armchair-shaped edge (AGNRs) can be either metallic or semiconducting depending on their width, and GNRs with a zigzag-shaped edge (ZGNRs) are metallic with peculiar edge states on both sides of the ribbon regardless of their width.[7,8] Recently, Son *et al.*[3] and Yang *et al.*[4] predicted that both AGNRs and ZGNRs are semiconductors with different band gaps for the same width. In addition, ZGNRs are predicted to be able to carry a spin current around the edge with dangling bonds, which makes them behave as a half metal, and have potential applications as nanosized spintronic devices.[2] Thus, the characterization of the edge structure is essential for GNR physics and applications.

Currently, atomic force microscope (AFM) is used to identify the thickness and width of GNRs.[1,5,6] However, it is difficult to get the information about the exact edge structure of GNRs since the radius of AFM tip is so large (>10 nm for Si_3N_4 tip) that atomic resolution can hardly be obtained. Raman spectroscopy is demonstrated to be a powerful and nondestructive tool to probe the structure of graphitic materials, such as pyrolytic graphite, fullerenes, carbon nanotubes, and graphene.[9–20] Especially, the defect-associated *D*-band signal can be observed only in an armchair edge (but not in a zigzag edge) since the intervalley double resonance scattering responsible for the origin of *D* band does (does not) occur.[13,14,19,20] Theoretical calculations also show that the zigzag and armchair edges of GNRs exhibit different localized vibrational modes (LVMs).[21–24] Thus, a direct comparison of calculations with Raman measurements is of great interest and will provide useful information for the characterization of GNRs by using Raman spectroscopy.

Recently, we developed a surface and interference co-enhanced Raman scattering (SICERS) technique,[25] which enables a strong Raman signal of individual mono- and few-layer GNRs with a width of 5 nm to hundreds of nanometers. In SICERS measurements, an optimized substrate of Si wafer capped with a 50-nm-thick Ag film and a 72-nm-thick Al_2O_3 top layer was used to support GNRs.[25] The Raman signals of GNRs can be remarkably enhanced by two enhancement factors: surface enhanced Raman spectroscopy by the Ag film and enhancement of electric field by interference with reflected light by the Al_2O_3 top layer.[25] In this study, we systematically investigated the Raman spectra of individual mono- and few-layer GNRs by using SICERS technique. Interestingly, the Raman features of individual mono- and few-layer GNRs obtained show two well-distinguished bands of 1450 and 1530 cm^{-1}, whose intensities are sensitive to the width and edge structure of GNRs. Combining with first-principles calculation results, these two bands are assigned to be the localized vibration of the edge atoms of zigzag and armchair GNRs terminated with H atoms, respectively. In addition, two weak peaks at ~1140 and 1210 cm^{-1} are also found, which are coupled with 1450 and 1530 cm^{-1}, respectively.

The presentation of this paper is organized as follows: Section II discusses the experimental details; Sec. III presents the experimental observations on the Raman spectra of mono- and few-layer GNRs, including the Raman spectra of individual mono- and few-layer GNRs and the effects of number of layers, ribbon width, and edge structure on the two peaks at 1450 and 1530 cm^{-1}; Sec. IV discusses the assignments of the above two peaks based on first-principles calculations and experimental observations; and Sec. V discusses the two small peaks at ~1140 and 1210 cm^{-1} observed from GNRs and the possible edge structure of GNRs. A conclusion is given in Sec. VI.

 ©2010 The American Physical Society

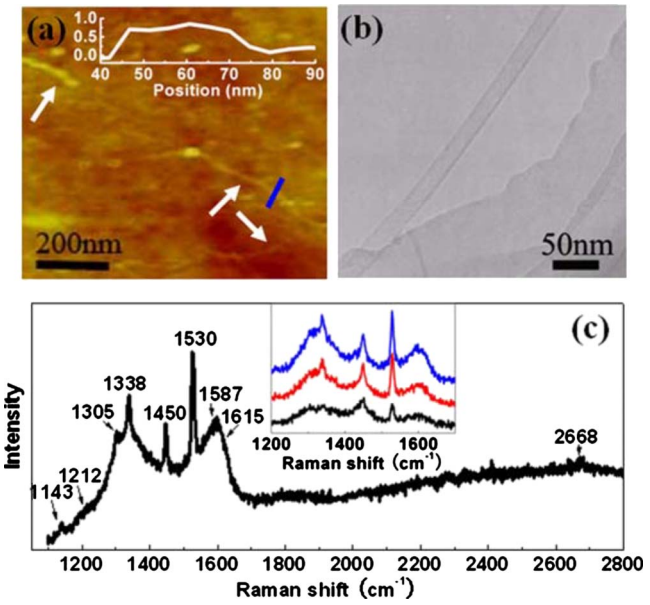


FIG. 1. (Color online) (a) AFM image, (b) TEM image, and (c) Raman spectra of chemically derived mono-layer GNRs. The GNRs in (a) are denoted by white arrows. The inset of (a) shows the cross section taken along the black line (blue line online), indicating that the thickness and width of the measured GNR are ~0.9 and ~20 nm, respectively. The inset of (c) shows the Raman spectra of three individual GNRs.

II. EXPERIMENT

Both mono- and few-layer GNR samples were used in our experiments. The mono-layer GNRs were fabricated by sonication cutting of graphene obtained by chemical exfoliation of artificial graphite,[26] similar to that reported by Li *et al.*[1] They have a width mostly in the range of 5–50 nm and length up to several micrometers. Moreover, ~75% of the chemically derived GNRs are mono-layers based on AFM observations. The few-layer GNRs were obtained by mechanical cleavage of highly oriented pyrolytic graphite with a Scotch tape,[27] and most of them are more than three layers, having a width typically from tens to hundreds of nanometers and a length of up to several micrometers.

For Raman measurements, the cleaved GNRs were transferred to a SICERS substrate,[25] and the supernatant containing the chemically derived GNRs was spin coated on a SICERS substrate. The Raman spectra of these GNR samples were measured and collected using 1.58, 1.96, and 2.41 eV lasers under ambient conditions. The laser spot size (~1 μm) used was much larger than the width of GNRs. All the ribbons were measured at a laser power below 1 mW and for a short collection time (120 s) in order to avoid possible sample damage or laser-induced heating.

III. EXPERIMENTAL OBSERVATIONS ON THE RAMAN SPECTRA OF INDIVIDUAL MONO- AND FEW-LAYER GNRS

Figure 1 shows the typical AFM image, transmission electron microscope (TEM) image, and Raman spectra of mono-layer GNRs with a width of 5–50 nm fabricated by chemical exfoliation of artificial graphite. Similar to chemically derived graphene, the G band (~1580 cm^{-1}), defect-related D band (~1300–1350 cm^{-1}), and D' band (~1615 cm^{-1}) are observed from these chemically derived GNRs. The G peak is due to the doubly degenerated zone-center E_{2g} mode, and the D and D' bands are related to the scattering of zone-boundary and zone-center phonons, respectively, with elastic scattering by defects in graphitic materials.[9,10,12–20] As a significant difference, we observed two well-distinguished additional peaks at 1450 and 1530 cm^{-1} with a very sharp (linewidth of ~7 cm^{-1} for both peaks) and symmetric Lorentzian shape. Considering the structural difference between graphene and GNRs, we consider that the two characteristic peaks may be correlated with the vibrations of edge atoms of GNRs.

In order to clarify the origin of the two peaks, we also measured the Raman spectra of mechanically cleaved few-layer GNRs. Figure 2(a) shows the optical image of cleaved few-layer graphenes and GNRs on a SICERS substrate. The visibility of few-layer GNRs allows us to specify isolated GNRs one by one during the Raman measurements. The large distance (>1 μm) between the GNRs ensures that the collected Raman signal is only from one isolated few-layer GNR. Estimated by AFM measurements [Fig. 2(b)], A, B, and C ribbons have the same thickness of ~3 nm (~8 layers) and widths of ~480, 230, and 110 nm, respectively. The same number of layers for these ribbons indicates that they were cleaved from the same graphite sheet. In combination with the parallel configuration for A, B, and C ribbons, we expect that these few-layer GNRs may have the same edge structure. The parallel configuration also avoids the effect of polarization on the Raman intensity of different GNRs. Thus, we consider that the different Raman features of A, B, and C GNRs may originate from their different widths.

Figure 2(c) shows the Raman spectra of the cleaved few-layer GNRs located at A, B, and C, in which their intensity is normalized by the G-band intensity. Similar to the cleaved graphene, the two most intense features are the G peak at ~1580 cm^{-1} and the $2D$ band at ~2700 cm^{-1}. In addition, the defect-related D band (~1300–1350 cm^{-1}) and D' band (~1615 cm^{-1}) are observed. Because of the high quality of cleaved graphene, the D band is usually observed at graphene edges with high intensity and is absent or very weak in the center of graphene layers.[15–17,19,20] The intensity ratio (I_D/I_G) of D to G band of the few-layer GNRs increases with decreasing the ribbon width from A to C because of the higher percentage of edges for narrower ribbons. Importantly, similar to the mono-layer GNRs, two well-distinguished additional peaks are observed at 1450 cm^{-1} (linewidth of ~7 cm^{-1}) and 1530 cm^{-1} (linewidth of ~8 cm^{-1}) in the Raman spectra of few-layer GNRs. Moreover, these two peaks appear at the same frequency for the GNRs with different numbers of layers (Fig. 3). This fact suggests that the influence of the number of layers (or layer coupling) on these two Raman modes is sufficiently small. The relative intensity of these two peaks to the G band increases with decreasing the ribbon width [Fig. 2(d)], consistent with the I_D/I_G evolution with the ribbon width. This

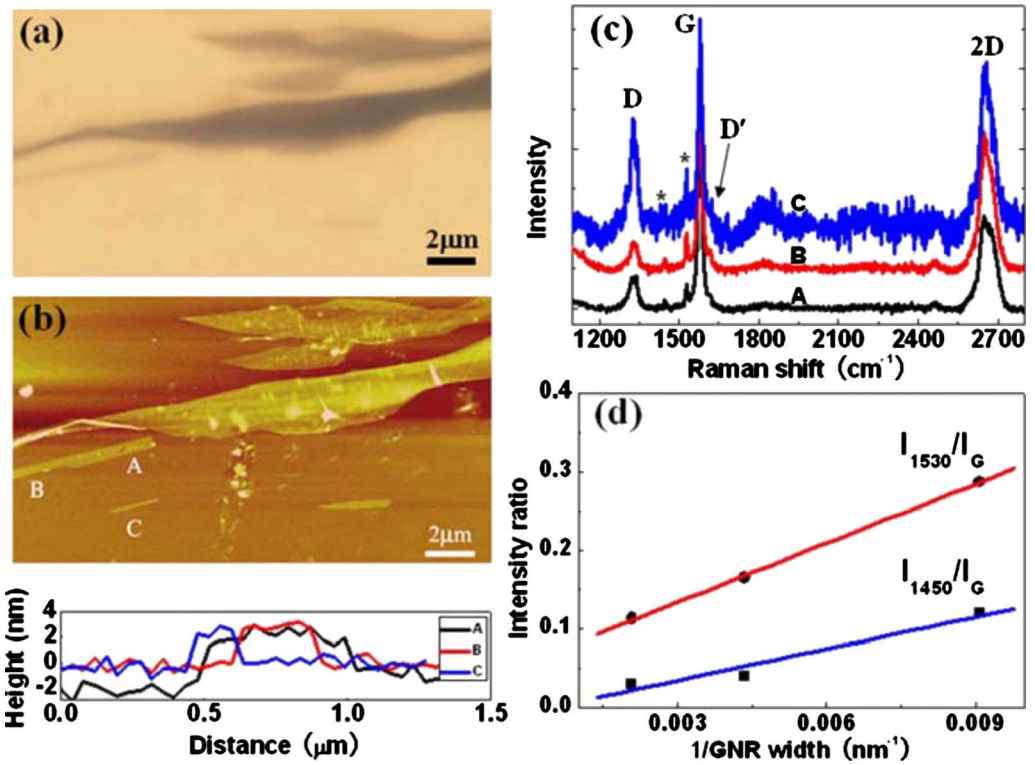


FIG. 2. (Color online) (a) Optical image and (b) the corresponding AFM image of cleaved few-layer graphene and GNRs. Bottom of the left panel shows their corresponding topographic profiles. (c) *G*-band intensity normalized Raman spectra of few-layer GNRs located at A, B, and C, with the two characteristic vibration modes at 1450 and 1530 cm^{-1} denoted by *. (d) The intensity ratio of 1530 and 1450 cm^{-1} to *G* band as a function of reciprocal GNR width.

further confirms that the two peaks of 1450 and 1530 cm^{-1} are the intrinsic feature of edge atoms of GNRs. Thus, these two peaks were also observed for the graphene with some GNRs on its surface.[25]

Compared with the Raman spectra of few-layer GNRs shown in Fig. 2, it is important to note that a further decrease in GNR width (~100 nm) leads to a significant increase in the relative intensity of 1450 and 1530 cm^{-1} bands to the *G* band [Fig. 1(c)]. According to the relationship presented in Fig. 2(d), the width of the chemically derived mono-layer GNRs is estimated to be ~20 nm, which is consistent with the mean width obtained by AFM measurements. Thus, the relative intensity of these signals to *G* band can be used to estimate the width of GNRs.

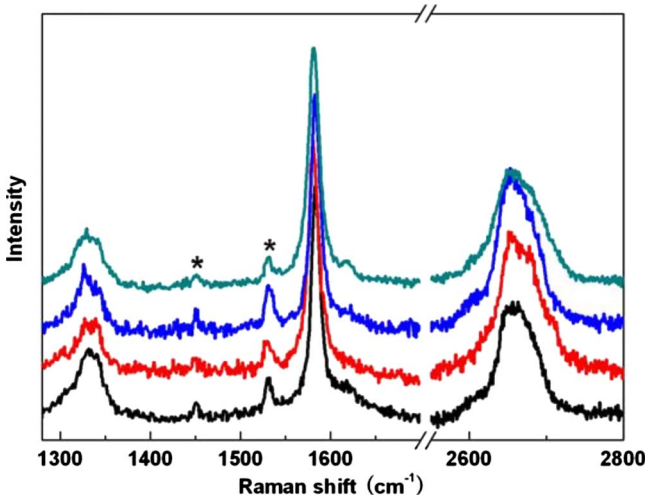


FIG. 3. (Color online) The influence of the number of layers of GNRs on their Raman spectra, with the two characteristic vibration modes at 1450 and 1530 cm^{-1} denoted by *. The corresponding numbers of layers are ~3, 6, 7, and 10 from the bottom to top, based on AFM measurements.

We also investigated the effect of edge structure on the two peaks at 1450 and 1530 cm^{-1}. Figure 4(a) shows the AFM image of an irregular few-layer GNR. It is considered that the appearance of zigzag and armchair edges should be different for the A, B, and C positions because of their different edge orientations. This structure allows us to investigate the effect of edge structure on the Raman spectra of few-layer GNRs. It is interesting to find that the relative intensity of 1530 to 1450 cm^{-1} (I_{1530}/I_{1450}) remarkably increases when the measurement location moves from the wedgelike structure (position A) to the regular ribbon (position C) [Fig. 4(b)]. A similar behavior was observed for the relative intensity of *D* band to 1450 cm^{-1} (I_D/I_{1450}) [Fig. 4(b)]. In addition, the Raman intensities I_D and I_{1530} are also correlated with each other for different samples of monolayer [inset of Fig. 1(c)] and few-layer GNRs [Figs. 4(c) and 4(d)]. This observation suggests that 1530 and 1450 cm^{-1} peaks are originated from different edge structures of GNRs, and *D* band and 1530 cm^{-1} may come from the same origin (armchair edge).[13,14,19,20]

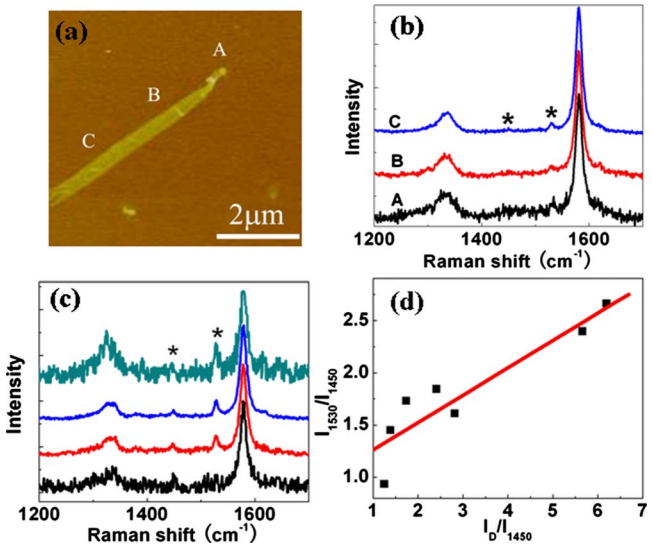


FIG. 4. (Color online) (a) AFM image of an irregular few-layer GNR, which exhibits different edge orientations at different regions. *G*-band intensity normalized Raman spectra of (b) different positions for the same GNR in (a) and of (c) different few-layer GNRs. * denotes the two characteristic vibration modes at 1450 and 1530 cm^{-1}. (d) I_{1530}/I_{1450} vs I_D/I_{1450} for the Raman spectra in (b) and (c).

IV. ASSIGNMENTS OF THE TWO RAMAN PEAKS AT 1450 AND 1530 cm^{-1}

In order to analyze the origin of the two characteristic bands at 1450 and 1530 cm^{-1}, we studied the vibrational properties of H-free and H-terminated AGNRs and ZGNRs (Fig. 5) by density-functional theory (DFT) calculation. The DFT calculations were performed by using the SIESTA code.[28] We used the Perdew-Burke-Ernzerhof generalized gradient approximation exchange correlation functional[29] and norm-conserving pseudopotentials.[30,31] Integration over the one-dimensional Brillouin zone was carried out by using the Monkhorst-Pack scheme, and 31 (for zigzag) and 21 (for armchair) *k* points were used in our calculations. All geometries were optimized until the forces on the atoms are smaller than 0.01 eV/Å. Here, we focus only on the edge localized vibrational modes. The reason is that the vibrational frequencies of edge phonons do not depend on the width of GNRs, and thus the observed Raman spectra will be sharp.

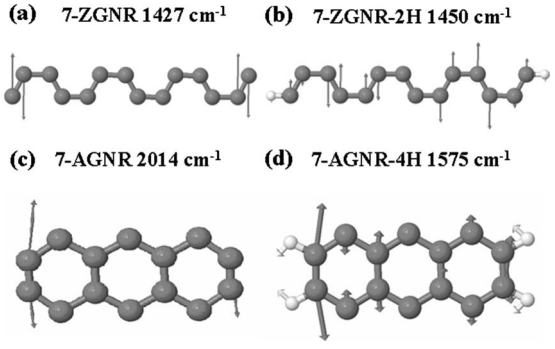


FIG. 5. Calculated edge phonon modes of (a) H-free 7-ZGNR, (b) H-terminated 7-ZGNR, (c) H-free 7-AGNR, and (d) H-terminated 7-AGNR. The number before the AGNR and ZGNR denotes the width of GNRs, which corresponds to the number of dimer lines across the ribbon width for AGNR and the number of zigzag chains across the ribbon width for ZGNR.

Consistent with our observations of the sharp *G*-band spectra (~1585 cm^{-1}) of GNRs (Figs. 1–4), the calculated results show that the *G* band can be found at a similar frequency (~1612 cm^{-1}) for all GNRs even though their width is very small because the *G* band is the optical phonon modes for neighbor atoms. Especially, we found several unique edge phonon states of GNRs since the edge atoms are reconstructed so as to minimize the surface energy. For the H-free ZGNRs, their edge C—C bond length (1.37 Å) is shorter than the normal one (1.42 Å). A localized edge phonon mode at ~1430 cm^{-1} is expected because one of the three C—C bonds is missing at the zigzag edge [Fig. 5(a)], which is consistent with the previous calculation (~1450 cm^{-1}) by Zhou and Dong.[23] Moreover, it is important to note that the LVM of H-terminated ZGNRs remains almost the same with that of H-free ZGNRs, with a frequency of ~1450 cm^{-1} [Fig. 5(b)], although the maximum amplitude of the phonon mode shifts to the inner region from the edge. Since the H termination of the edge atoms does not change the sp^2 hybridization of the C—C bond at the zigzag edges, the edge phonon mode of 1450 cm^{-1} observed for ZGNRs does not depend much on the H termination.

However, in the case of H-free AGNRs [Fig. 5(c)], the reconstruction of the edge atom leads to a great decrease in the length of edge bonds (~1.23 Å), which are supposed to be a C≡C triple bond. Thus a higher-frequency Raman peak at ~2000 cm^{-1} is obtained to be related to the LVM of the edge atoms [Fig. 5(c)], which is consistent with Ref. 23 and the Raman spectra of carbon chain $C_{10}H_2$ in a single-walled carbon nanotubes (~2066 cm^{-1}).[32] However, the C≡C triple bond for H-free AGNRs becomes C=C double bond when hydrogen atoms are attached on their edges. In this case, the edge phonon mode becomes close to the *G* band because the original edge bond in the H-free AGNRs becomes longer (~1.39 Å) and the total mass of edge atoms is increased after saturating H atoms. When we assume that C—H bond is sufficiently strong compared with hydrogen mass, we can consider that the edge C atom changes the atomic weight from 12 (C) to 13 (C+H). The corresponding edge phonon frequency should change to $1580\times(12/13)^{1/2}$ ~1530 cm^{-1}. The calculated result shows that a LVM at ~1575 cm^{-1} appears for the H-terminated AGNRs [Fig. 5(d)], which is lower than the calculated *G*-band frequency (1612 cm^{-1}).

Experimentally it is very difficult to obtain GNRs with free edges under ambient and solution conditions for the present preparation methods. Thus, we assign the 1530 cm^{-1} peak to the LVM of armchair edge with a terminated H atom per C atom. This is consistent with the above observations about the intensity correlation between 1530 cm^{-1} band and armchair edge-related *D* band (Fig. 4). The frequency deviation between the experimentally observed (~1530 cm^{-1}) and theoretically predicted (~1575 cm^{-1}) LVMs is within the accuracy of the calculation (~30 cm^{-1}). Due to the same

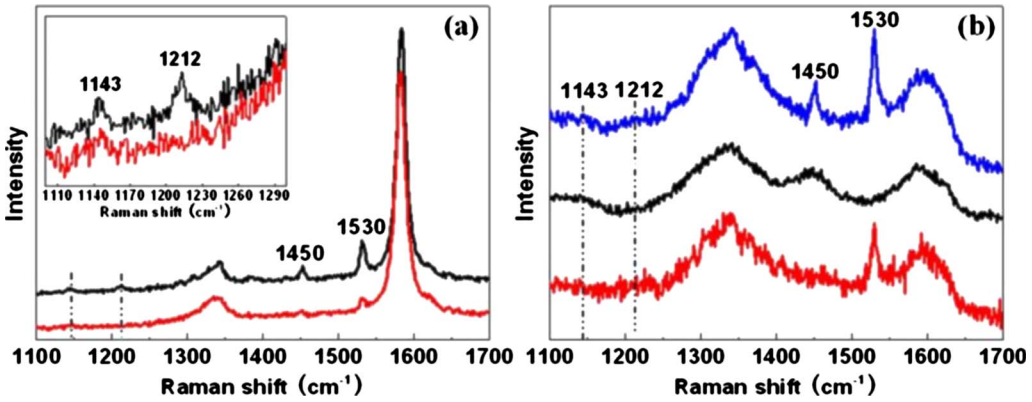


FIG. 6. (Color online) (a) Raman spectra of few-layer GNRs with different intensity ratios of 1450 to 1530 cm^{-1}. The inset shows the enlarged spectra in the range of 1100–1300 cm^{-1}. (b) Raman spectra of mono-layer GNRs with different intensity ratios of 1450 to 1530 cm^{-1} on Si/300 nm SiO_2 substrate. The dashed lines are used to show the positions of 1143 and 1212 cm^{-1} peaks.

preparation method and the same frequency with the predicted LVM of H-terminated ZGNRs, the 1450 cm^{-1} peak is assigned to be the edge phonon mode of H-terminated ZGNRs. We note that the 1450 cm^{-1} peak was previously assigned to the multiorder of silicon substrate or poly(methyl methacrylate) (PMMA) (Refs. 19 and 33); however, it is not true in our case since this peak cannot be observed in the bare area of the same substrate with the same measurement conditions (see supplementary material[34]) and no any PMMA was used in our experiments. The above assignments of these two peaks to the localized vibrations of edge atoms are consistent with their very narrow spectral width (~7 cm^{-1}).

From the above results, we can distinguish the orientation of the ribbon edge by Raman spectroscopy as well as define the local degree of order of the atomic structure at the edge of GNRs according to the relative intensity of 1450 to 1530 cm^{-1}. Furthermore, this technique is more sensitive than *D* band since *D* band is generally broad and all kinds of defects that can break the symmetry and selection rule contribute to the *D*-band intensity as well. The coexistence of the two peaks for an isolated GNR in Figs. 1–4 may suggest the imperfection of the edge structure.

V. TWO SMALL RAMAN PEAKS AND THE EDGE STRUCTURE OF GNRS

In addition to the well-distinguished 1450 and 1530 cm^{-1} peaks, two very weak peaks at ~1140 and ~1210 cm^{-1} are found for the mono- and few-layer GNRs (Figs. 1, 2, and 6). Moreover, the intensities of 1140 and 1210 cm^{-1} peaks are correlated with the intensities of 1450 and 1530 cm^{-1} peaks, respectively. No obvious peaks at ~1140 and 1210 cm^{-1} are found in the Raman spectra with very low 1450 and 1530 cm^{-1} peaks (see supplementary material[34]). In addition, the relative intensity of 1140 and 1210 cm^{-1} peaks to *G* band increases with decreasing the ribbon width [Fig. 2(c)], similar to the behavior of 1450 and 1530 cm^{-1} peaks, which indicates that these two peaks are also related to the edge phonons of GNRs. Considering the much lower intensities of these two peaks compared to 1450 and 1530 cm^{-1} peaks, we selected the Raman spectra with well-defined spectral features at ~1140 and 1210 cm^{-1} to determine the relation between these two peaks and 1450 and 1530 cm^{-1} peaks. Figure 6(a) shows two Raman spectra of few-layer GNRs with different intensity ratios of 1530 to 1450 cm^{-1}. It is clearly seen that the 1210 cm^{-1} peak becomes clear with increasing the intensity ratio of 1530 to 1450 cm^{-1}. Moreover, the same behavior was also observed for ~1140 and ~1210 cm^{-1} peaks of mono-layer GNRs on a commonly used substrate of Si/300 nm SiO_2 [Fig. 6(b)] although the signals are not so clear. These results suggest that the 1140 and 1210 cm^{-1} peaks are coupled with 1450 and 1530 cm^{-1}, respectively.

It is interesting to note that the above observations on GNRs terminated by H atoms are very similar to those reported for polyacetylene.[35–37] *Trans*-polyacetylene usually shows two peaks at ~1150 and 1450 cm^{-1},[35,36] and *cis*-polyacetylene shows two peaks at ~1240 and 1540 cm^{-1}.[37] It is well known that polyacetylene is a long chain of carbon atoms with alternating single and double bonds between them, each with one H atom.[38] Importantly, *trans*- and *cis*-polyacetylene have zigzag and armchair structures,[38] respectively, which are similar to the edge structure of H-terminated ZGNRs and AGNRs. Thus, the similarity in the Raman features between GNRs and polyacetylene further confirms our assignments on the two peaks at 1450 and 1530 cm^{-1} observed from GNRs. That is, 1450 and 1530 cm^{-1} peaks physically originate from the localized vibration of the edge atoms of zigzag and armchair GNRs terminated with H atoms, respectively.

It has been well established that the optical energy gap is ~1.6 eV for *trans*-polyacetylene and 1.9–2.1 eV for *cis*-polyacetylene.[38] Moreover, the band gap of polyacetylene increases as the effective conjugation length decreases.[36] Thus, the similar edge structure of H-terminated GNRs with polyacetylene leads to an interesting observation of the resonance effect of the two well-distinguished 1450 and 1530 cm^{-1} peaks of GNRs. Figure 7 shows Raman spectra of few-layer GNRs within 1200–1700 cm^{-1} excited by lasers of 1.58, 1.96, and 2.41 eV. It is interesting to note that 1450 and 1530 cm^{-1} peaks can be observed by an excitation laser of 1.96 eV but not by excitation lasers of 1.58 and 2.41 eV. Although the enhancement of SCIERS is laser wave-

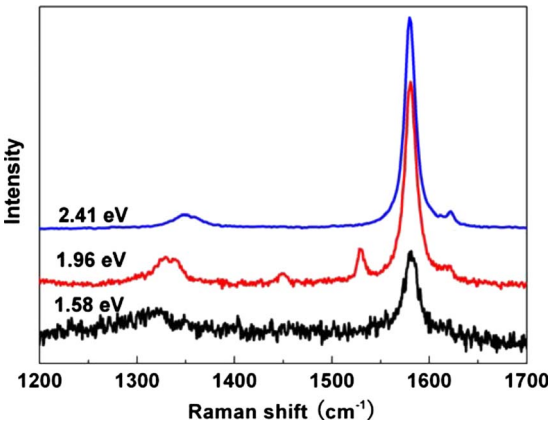


FIG. 7. (Color online) Raman spectra of few-layer GNRs excited by laser energies of 1.58, 1.96, and 2.41 eV.

length dependent,[25,39] strong Raman signals and good signal/noise ratio were obtained for 2.41 eV laser. Thus, the suppression of 1450 and 1530 cm^{-1} peaks in the cases of 1.58 and 2.41 eV lasers cannot be attributed to the low signal quality, but possibly due to the lack of resonance conditions for H-terminated armchair and zigzag edges with a specific length in the GNRs studied. Further studies about the laser energy dependence of 1450 and 1530 cm^{-1} peaks by using an excitation laser with energy around 1.9 eV or tunable laser are required for further understanding the edge structure of GNRs in the future.

VI. CONCLUSION

We observed two well-distinguished bands of 1450 and 1530 cm^{-1} in the Raman spectra of individual mono- and few-layer GNRs by using surface and interference coenhanced Raman scattering technique. Their intensities are sensitive to the width and edge structure of GNRs. Combining with first-principles calculations, these two bands are assigned to be correlated with the localized edge phonon mode of zigzag and armchair GNRs terminated with H atoms, respectively. In addition, two weak peaks at ~1140 and 1210 cm^{-1} are also found, which are coupled with 1450 and 1530 cm^{-1}, respectively. These findings open up a possibility to characterize the width and fine edge structure of GNRs by using Raman spectroscopy, will be helpful for the controllable synthesis of GNRs, and accordingly facilitate the property investigations and applications of GNRs.

ACKNOWLEDGMENTS

This work was supported by NSFC (Contracts No. 50972147, No. 50872136, No. 50921004, and No. 50702063) and CAS (Contract No. KJCX2-YW-231). R.S. acknowledges MEXT (Grant No. 20241023).

*wcren@imr.ac.cn
†cheng@imr.ac.cn

[1] X. L. Li, X. R. Wang, L. Zhang, S. W. Lee, and H. J. Dai, Science **319**, 1229 (2008).
[2] Y. W. Son, M. L. Cohen, and S. G. Louie, Nature (London) **444**, 347 (2006).
[3] Y. W. Son, M. L. Cohen, and S. G. Louie, Phys. Rev. Lett. **97**, 216803 (2006).
[4] L. Yang, C. H. Park, Y. W. Son, M. L. Cohen, and S. G. Louie, Phys. Rev. Lett. **99**, 186801 (2007).
[5] M. Y. Han, B. Ozyilmaz, Y. B. Zhang, and P. Kim, Phys. Rev. Lett. **98**, 206805 (2007).
[6] X. R. Wang, Y. J. Ouyang, X. L. Li, H. L. Wang, J. Guo, and H. J. Dai, Phys. Rev. Lett. **100**, 206803 (2008).
[7] M. Fujita, K. Wakabayashi, K. Nakada, and K. Kusakabe, J. Phys. Soc. Jpn. **65**, 1920 (1996).
[8] K. Nakada, M. Fujita, G. Dresselhaus, and M. S. Dresselhaus, Phys. Rev. B **54**, 17954 (1996).
[9] R. Saito, G. Dresselhaus, and M. S. Dresselhaus, *Physical Properties of Carbon Nanotubes* (Imperial College Press, London, 1998).
[10] R. Saito, A. Jorio, A. G. Souza, G. Dresselhaus, M. S. Dresselhaus, and M. A. Pimenta, Phys. Rev. Lett. **88**, 027401 (2001).
[11] A. Jorio, R. Saito, J. H. Hafner, C. M. Lieber, M. Hunter, T. McClure, G. Dresselhaus, and M. S. Dresselhaus, Phys. Rev. Lett. **86**, 1118 (2001).
[12] M. S. Dresselhaus, G. Dresselhaus, R. Saito, and A. Jorio, Phys. Rep. **409**, 47 (2005).
[13] L. G. Cancado, M. A. Pimenta, B. R. A. Neves, M. S. S. Dantas, and A. Jorio, Phys. Rev. Lett. **93**, 247401 (2004).
[14] M. A. Pimenta, G. Dresselhaus, M. S. Dresselhaus, L. G. Cancado, A. Jorio, and R. Saito, Phys. Chem. Chem. Phys. **9**, 1276 (2007).
[15] A. C. Ferrari, J. C. Meyer, V. Scardaci, C. Casiraghi, M. Lazzeri, F. Mauri, S. Piscanec, D. Jiang, K. S. Novoselov, S. Roth, and A. K. Geim, Phys. Rev. Lett. **97**, 187401 (2006).
[16] A. C. Ferrari, Solid State Commun. **143**, 47 (2007).
[17] A. Gupta, G. Chen, P. Joshi, S. Tadigadapa, and P. C. Eklund, Nano Lett. **6**, 2667 (2006).
[18] A. Das, S. Pisana, B. Chakraborty, S. Piscanec, S. K. Saha, U. V. Waghmare, K. S. Novoselov, H. R. Krishnamurthy, A. K. Geim, A. C. Ferrari, and A. K. Sood, Nat. Nanotechnol. **3**, 210 (2008).
[19] C. Casiraghi, A. Hartschuh, H. Qian, S. Piscanec, C. Georgi, A. Fasoli, K. S. Novoselov, D. M. Basko, and A. C. Ferrari, Nano Lett. **9**, 1433 (2009).
[20] L. M. Malard, M. A. Pimenta, G. Dresselhaus, and M. S. Dresselhaus, Phys. Rep. **473**, 51 (2009).
[21] M. Igami, M. Fujita, and S. Mizuno, Appl. Surf. Sci. **130-132**, 870 (1998).
[22] T. Kawai, Y. Miyamoto, O. Sugino, and Y. Koga, Phys. Rev. B **62**, R16349 (2000).
[23] J. Zhou and J. M. Dong, Appl. Phys. Lett. **91**, 173108 (2007).
[24] T. Tanaka, A. Tajima, R. Moriizumi, M. Hosoda, R. Ohno, E. Rokuta, C. Oshima, and S. Otani, Solid State Commun. **123**, 33 (2002).
[25] L. B. Gao, W. C. Ren, B. L. Liu, R. Saito, Z. S. Wu, S. S. Li, C.

B. Jiang, F. Li, and H. M. Cheng, ACS Nano **3**, 933 (2009).
[26] Z. S. Wu, W. C. Ren, L. B. Gao, B. L. Liu, J. P. Zhao, and H. M. Cheng, Nano Res. (to be published).
[27] K. S. Novoselov, A. K. Geim, S. V. Morozov, D. Jiang, Y. Zhang, S. C. Dubonos, I. V. Grigorieva, and A. A. Fisov, Science **306**, 666 (2004).
[28] D. Sanchez-Portal, P. Ordejon, E. Artacho, and J. M. Soler, Int. J. Quantum Chem. **65**, 453 (1997).
[29] J. P. Perdew, K. Burke, and M. Ernzerhof, Phys. Rev. Lett. **77**, 3865 (1996); **78**, 1396 (1997).
[30] N. Troullier and J. L. Martins, Phys. Rev. B **43**, 1993 (1991).
[31] L. Kleinman and D. M. Bylander, Phys. Rev. Lett. **48**, 1425 (1982).
[32] D. Nishide, H. Dohi, T. Wakabayashi, E. Nishibori, S. Aoyagi, M. Ishida, S. Kikuchi, R. Kitaura, T. Sugai, M. Sakata, and H. Shinohara, Chem. Phys. Lett. **428**, 356 (2006).
[33] L. Y. Jiao, L. Zhang, X. R. Wang, G. Diankov, and H. J. Dai, Nature (London) **458**, 877 (2009).
[34] See supplementary material at http://link.aps.org/supplemental/10.1103/PhysRevB.81.035412 for Raman spectra of bare areas in the substrate and few-layer GNRs with very low 1450 and 1530 cm^{-1} peaks.
[35] T. Lopez-Rios, E. Sandre, S. Leclercq, and E. Sauvain, Phys. Rev. Lett. **76**, 4935 (1996).
[36] A. C. Ferrari and J. Robertson, Phys. Rev. B **63**, 121405(R) (2001).
[37] S. Lefrant, L. S. Lichtmann, H. Temkin, D. B. Fitchen, D. C. Miller, G. E. Whitwell II, and J. M. Burlitch, Solid State Commun. **29**, 191 (1979).
[38] L. Lauchlan, S. Etemad, T. C. Chung, A. J. Heeger, and A. G. MacDiarmid, Phys. Rev. B **24**, 3701 (1981).
[39] G. Xu, M. Tazawa, P. Jin, S. Nakao, and K. Yoshimura, Appl. Phys. Lett. **82**, 3811 (2003).